Electronic Supplementary Information

Free-standing micropatternable nanocomposites as efficient colour converting filters for light emitting devices

Paola Pareo,[a] Luigi Carbone,[b*] Fabrizio Mariano,[b] Antonella Zacheo,[b] Gianluca Accorsi,[b] Valentina Arima,[b] Giuseppe Gigli [b] and Michele Manca [a*]

[a] Fondazione Istituto Italiano di Tecnologia (IIT) - Center for Biomolecular Nanotechnologies (CBN) – Via Barsanti snc – 73010 , Arnesano (LE) - ITALY

[b] CNR NANOTEC-Istituto di Nanotecnologia U.O. Lecce, c/o Polo di Nanotecnologia-Campus Ecotekne, Via Monteroni-73100 , Lecce - ITALY

*corresponding authors e-mail: luigi.carbone@nanotec.cnr.it ; michele.manca@iit.it

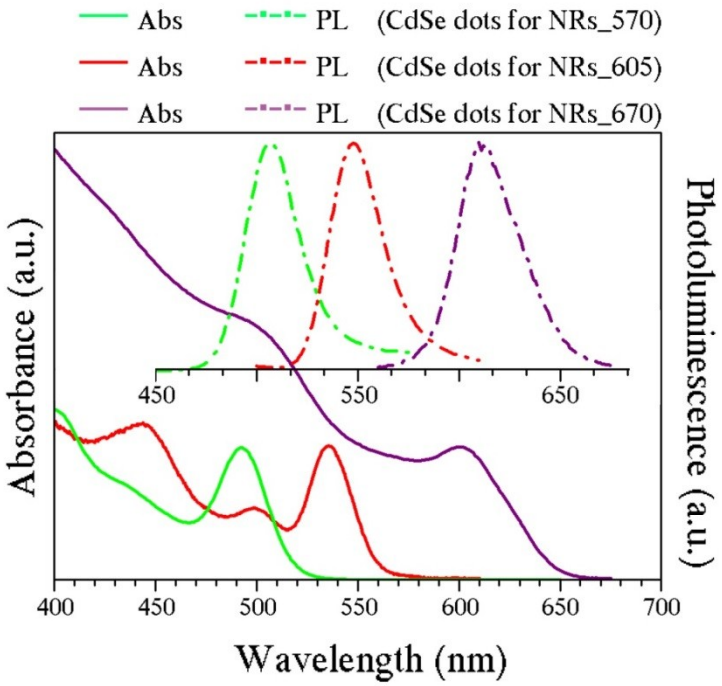

Figure S1. Absorption and photoluminescence spectra of toluene-dispersed CdSe dots lately employed in the syntheses of CdSe/CdS core/shell NRs. The spectra have been intensity-rescaled uniquely for graph appearance purposes.

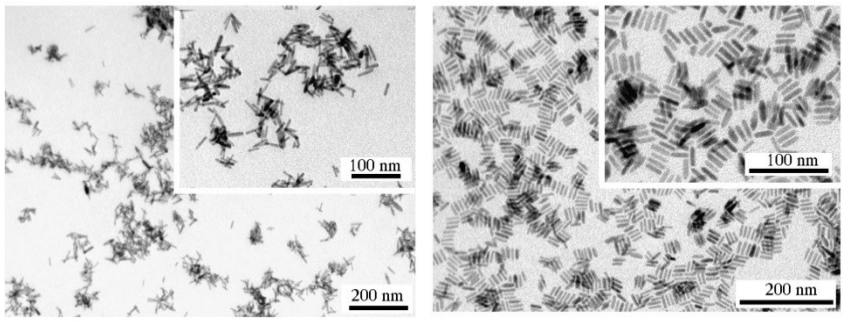

Figure S2. TEM micrographs of NRs_605/PMMA nanocomposite films at NRs weight concentrations respectively of 1.5wt%, 3wt%, (from left to right). Insets in the pictures report TEM images of samples at higher magnifications.

The confocal microscope was further used to examine the distribution of NRs throughout the entire plates by individually imaging multiple optical sections which were then accumulated to produce a 3D depth profile of the entire film thickness, as seen in the insets of Fig. S3. From these fluorescent confocal images it can be seen that the nanoparticles are dispersed relatively evenly throughout the thickness of the plates; however some agglomeration is observed, at high NR concentration.

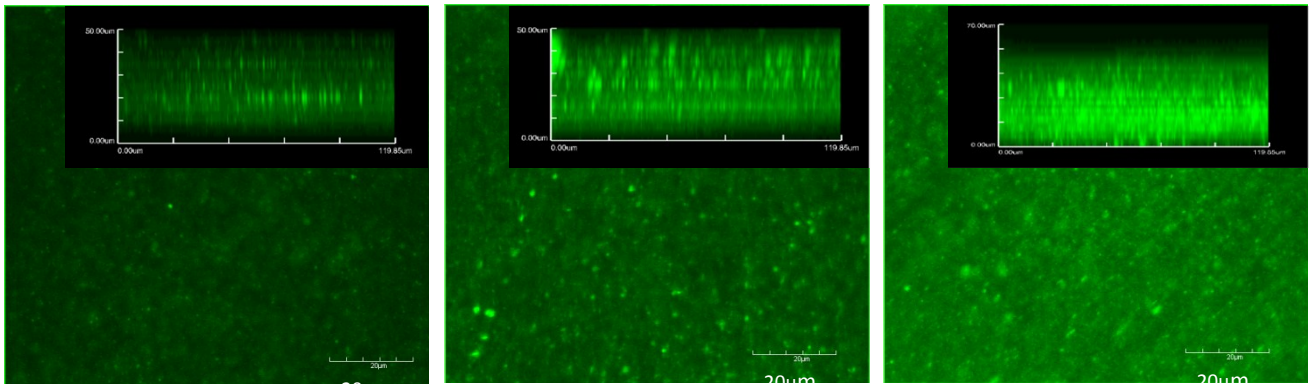

Figure S3. Confocal images of top views of NRs_605/PMMA NCP foils at NRs weight concentrations respectively of 0.2, 0.5 and 1wt% (from the left to the right side). Insets in the pictures report cross-sectional views of samples.

In the latter case, ultrathin sections of the nanocomposites were microtomed along the thickness direction and then laid on the copper grids in dry state in order to be TEM characterized. TEM images (Fig. S4) show an overview of the thin slices in which the electron dense NRs can be observed, confirming their presence within the NCP across the full thickness of the drop-casted and hot-embossed plates.

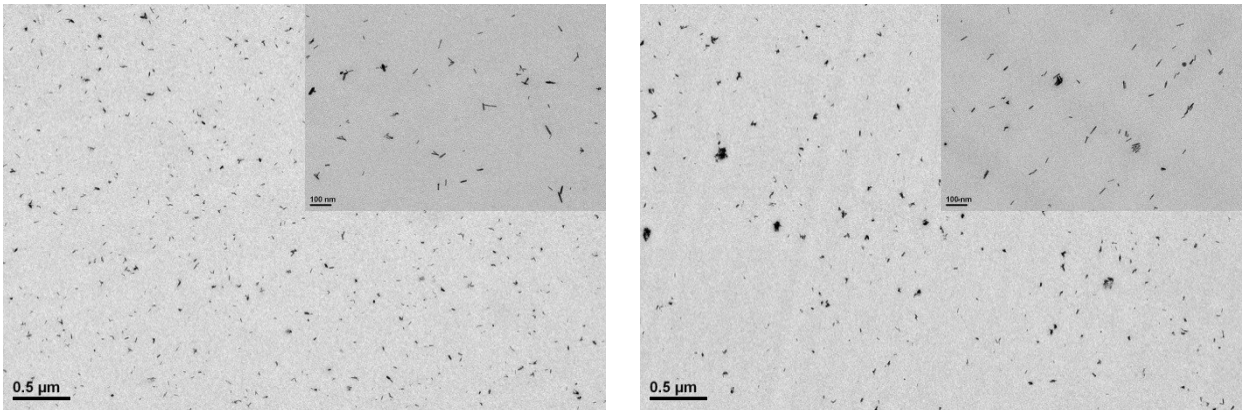

Figure S4. TEM images of cross-section of drop-cast NCP plates (on the left) and hot-embossed NCP plates (on the right), at 1wt% concentration of NRs_605/PMMA. Insets report TEM images of samples at higher magnifications.

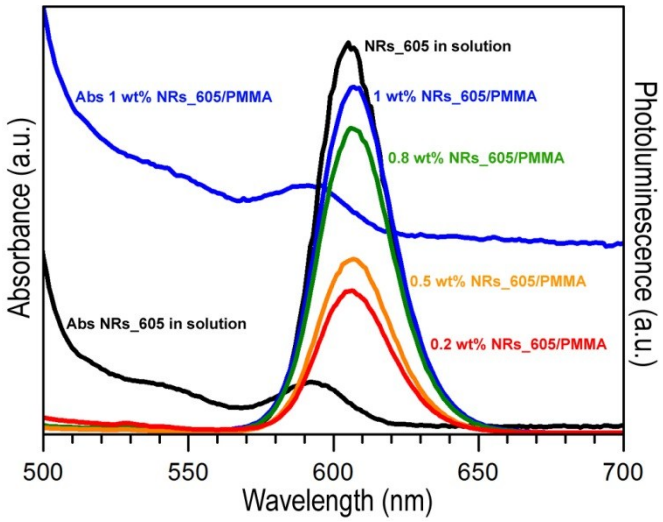

Figure S5. Absorption and photoluminescence spectra of NRs_605 in toluene-based solution (black lines) and in the PMMA-based NCP at different NRs weight amounts. The spectra have been intensity-rescaled uniquely for graph appearance purposes.

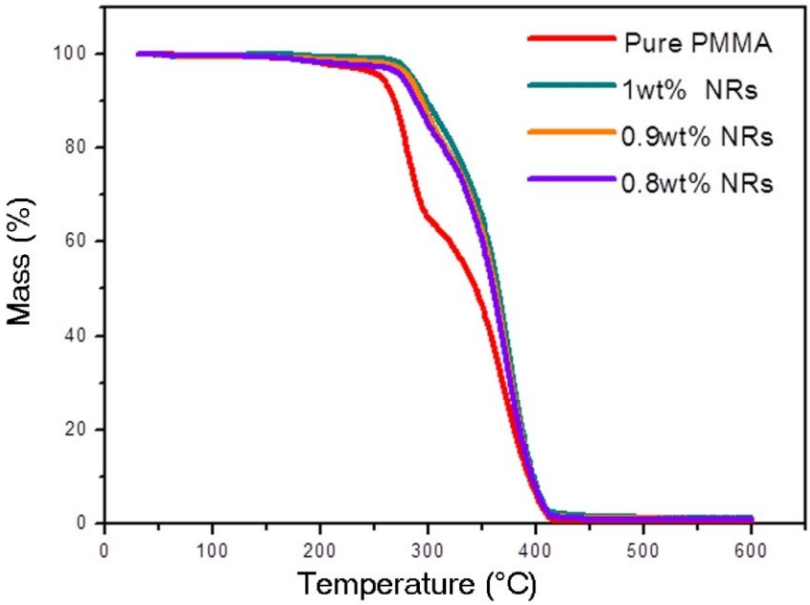

Figure S6. Thermogravimetric plots of three NCP samples embedded three different NR_605 concentrations compared with bare PMMA.

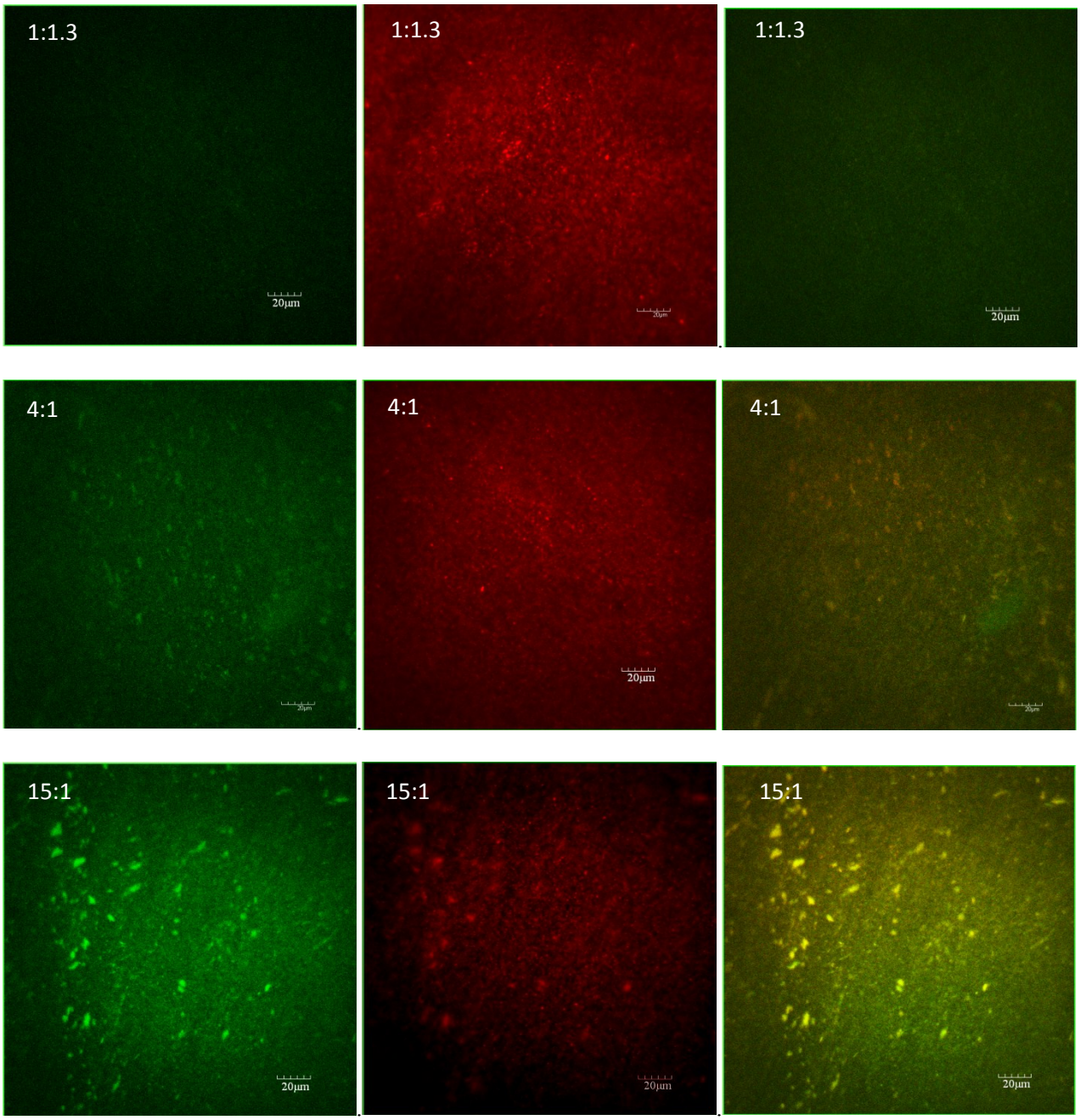

Figure S7. Confocal images of 150µm-thick nanocomposite plates obtained by two species of NRs. NRs_570-to-NRs_670 weight ratios are reported on top of pictures. Pictures of left line correspond to emission signals obtained by detection of only NRs_570 PL; pictures of middle line correspond to only NRs_670 emission signals, whereas the right line reports the emission from both NRs.

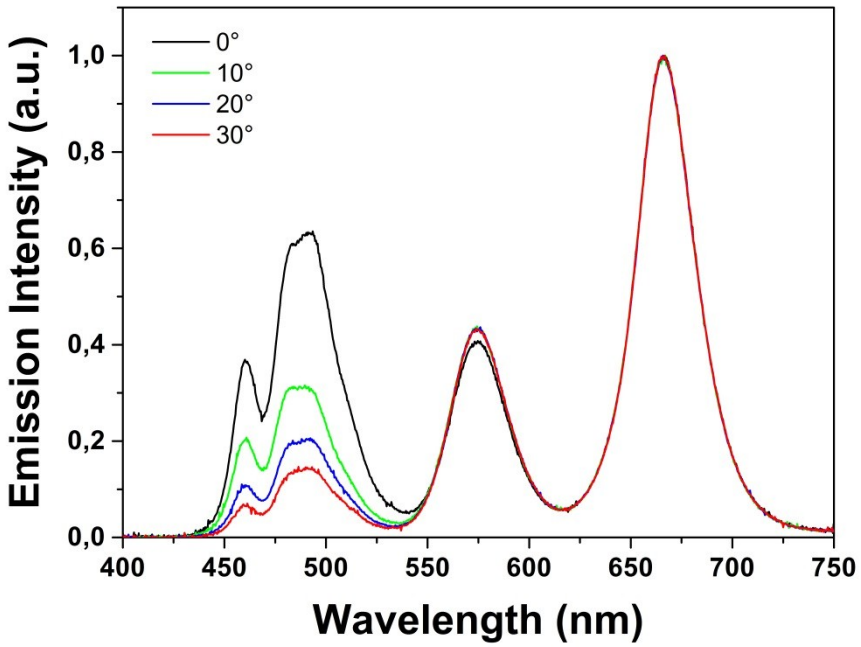

Figure S8. Light-emission spectra of the LED + stack #4 measured at four different viewing angles